

## Optimization of P-type poly-Si thermoelectric films design

Hyunse Kim\*, Yanglae Lee and Kong Hoon Lee

*Energy Systems Research Center, Korea Institute of Machinery and Materials,  
171 Jang-Dong, Yuseong-Gu, Daejeon, 305-343, South Korea*

(Manuscript Received April 5, 2007; Revised September 21, 2007; Accepted September 27, 2007)

---

### Abstract

In this study, a polycrystalline silicon (poly-Si) film layer for micro thermoelectric generators (TEGs) was optimized by using Taguchi methods. An experimental plan using an orthogonal array  $L_9 (3^4)$  is described. The fabrication process of the thermoelectric poly-Si films layer is presented in detail. The P-type poly-Si films were fabricated on a tetra ethoxy silane (TEOS) layer with a supporting Si wafer. The thermoelectric properties, Seebeck coefficient and electrical conductivity were measured, including the transport properties such as the hall coefficient, hall mobility and carrier concentration. The design parameters were optimized based on the experimental results. Using the optimum values, a p-type poly-Si films layer was fabricated and its power factor was measured. The measured power factor was  $541 \mu\text{Wm}^{-1}\text{K}^{-2}$ , which was better than the predicted value of  $221 \mu\text{Wm}^{-1}\text{K}^{-2}$ .

*Keywords:* Micro thermoelectric generator; poly-Si film; Taguchi methods

---

### 1. Introduction

Micro TEGs are regarded as important energy sources for mobile applications. Batteries are convenient but their duration time is very short. Fuel cells were once proposed as an alternative portable power source but, in this case, the electrical energy is generated from a chemical reaction, so there are byproducts such as water. Recently, micro TEGs were suggested as a safe and durable energy source [1-5]. Seiko Inc. commercialized wristwatches using a micro TEG. The watch works with  $1 \mu\text{W}$  of power generated from the temperature gradient between the body and environment. The main thermoelectric part is composed of a bismuth telluride (BiTe) thermoelectric layer, but it is not considered to be complementary metal oxide semiconductor (CMOS) process compatible material.

As a CMOS process compatible thermoelectric material, poly-Si is the main candidate. We are developing micro TEGs using poly-Si films, the output power of which is expected to be up to  $1 \text{ mW}/\text{cm}^2$ . It will be

applied to operate mobile equipment.

In designing micro poly-Si TEGs, the design parameters should be optimized to maximize the system performance. Taguchi methods are widely used for the optimization of mechanical system designs [6]. While conventional experimental studies are based on the classical full factorial approach, Taguchi methods adapt orthogonal arrays for designing efficient experiments and analyzing experimental data. Orthogonal arrays greatly reduce the size of experiments, as will be explained in the next paragraph. Recently, the application of Taguchi methods to the optimization of micro systems and micro fabrications was reported [7-8]. In this work, the poly-Si films layer used for the micro TEGs were designed by using Taguchi methods. The design parameters for the fabrication of the thermoelectric films were optimized with Taguchi methods. The experimental plan and fabrication processes are explained and the results are discussed.

### 2. Taguchi optimization

The crucial part of the micro TEG is the thermoelectric layer. The major properties of the thermoelec-

---

\*Corresponding author. Tel.: +82 42 868 7967, Fax.: +82 42 868 7355

E-mail address: hkim@kimm.re.kr

DOI 10.1007/s12206-007-1037-2

tric layer are the Seebeck coefficient and electrical conductivity. The thermoelectric power factor, TPF, can be obtained from the following equation:

$$\text{TPF} = \alpha^2 \times \sigma \quad (1)$$

where  $\alpha$  and  $\sigma$  are the Seebeck coefficient and the electrical conductivity, respectively. The TPF mainly affects the thermoelectric material's efficiency.

In this experiment, four design parameters for the fabrication of the micro TEG were chosen. Noise factors were not considered in this study. The design parameters are the thickness of a TEOS layer, the thickness of the poly-Si layer, the amount of energy in the ion-implantation process and the dose of boron ions. Each parameter has three possible values. The thickness of the TEOS layer was increased from 0.2  $\mu\text{m}$  to 0.4  $\mu\text{m}$  in steps of 0.1  $\mu\text{m}$ , and the three thicknesses of the poly-Si layer were 1.0  $\mu\text{m}$ , 1.5  $\mu\text{m}$  and 2.0  $\mu\text{m}$ , respectively. To fabricate p-type thermoelectric films, boron ions were implanted in poly-Si films. The supplied energy was varied from 30 keV to 50 keV and the dose was varied from  $10^{14} \text{ cm}^{-2}$  to  $10^{16} \text{ cm}^{-2}$ . The design parameters and values are explained in Table 1.

Generally, 81 (=  $3^4$ ) experiments are required to

Table 1. The design parameters and values.

Parameter	A TEOS Thickness ( $\mu\text{m}$ )	B Poly-Si Thickness ( $\mu\text{m}$ )	C Energy (keV)	D Dopant Dose ( $\text{cm}^{-2}$ )
Level 1	0.2	1.0	30	$10^{14}$
Level 2	0.3	1.5	40	$10^{15}$
Level 3	0.4	2.0	50	$10^{16}$

Table 2. The orthogonal array  $L_9$  ( $3^4$ ) from the Taguchi methodology.

Parameter	A TEOS Thickness	B Poly-Si Thickness	C Energy	D Dopant Dose
1	1	1	1	1
2	1	2	2	2
3	1	3	3	3
4	2	1	2	3
5	2	2	3	1
6	2	3	1	2
7	3	1	3	2
8	3	2	1	3
9	3	3	2	1

find the optimal values of four parameters of three levels. However, by adopting the orthogonal array  $L_9$  ( $3^4$ ) obtained from the Taguchi methodologies, nine sets of experiments are enough [9]. The orthogonal arrays of each parameter level for the experiment are listed in Table 2. A primary advantage of this orthogonal array is the relationship among the factors under investigation. For each level of any one factor, all levels of the other factors occur in an equal number of times, which can be noticed from the table. This constitutes a balanced experiment and permits the effect of one factor under study to be separable from the effect of the other factors. An additional advantage of the orthogonal array is its cost efficiency. Although balanced, the design of the orthogonal array does not require that all combinations of all factors be tested.

### 3. Fabrication

To perform the experiment, nine wafers were fabricated with different conditions based on the experimental plan. The processes are illustrated in Fig. 1. The fabrication process started from four-inch 525  $\mu\text{m}$  Si wafers, which were p-type and (1 0 0) oriented. The bare Si wafers were cleaned with ammonium peroxide mixture (APM) solution, followed by 30 seconds of HF cleaning. TEOS was deposited by using the low pressure chemical vapor deposition

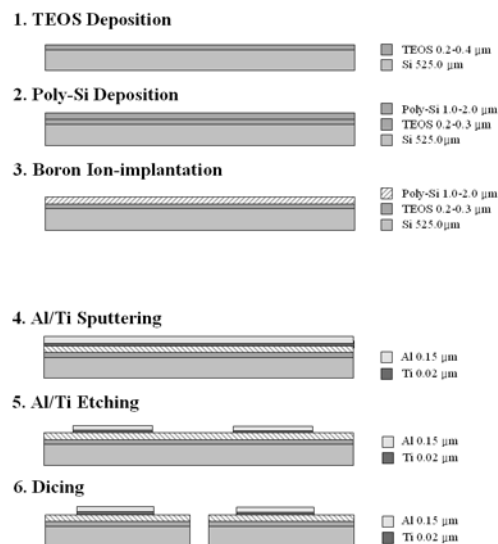


Fig. 1. Fabrication process.

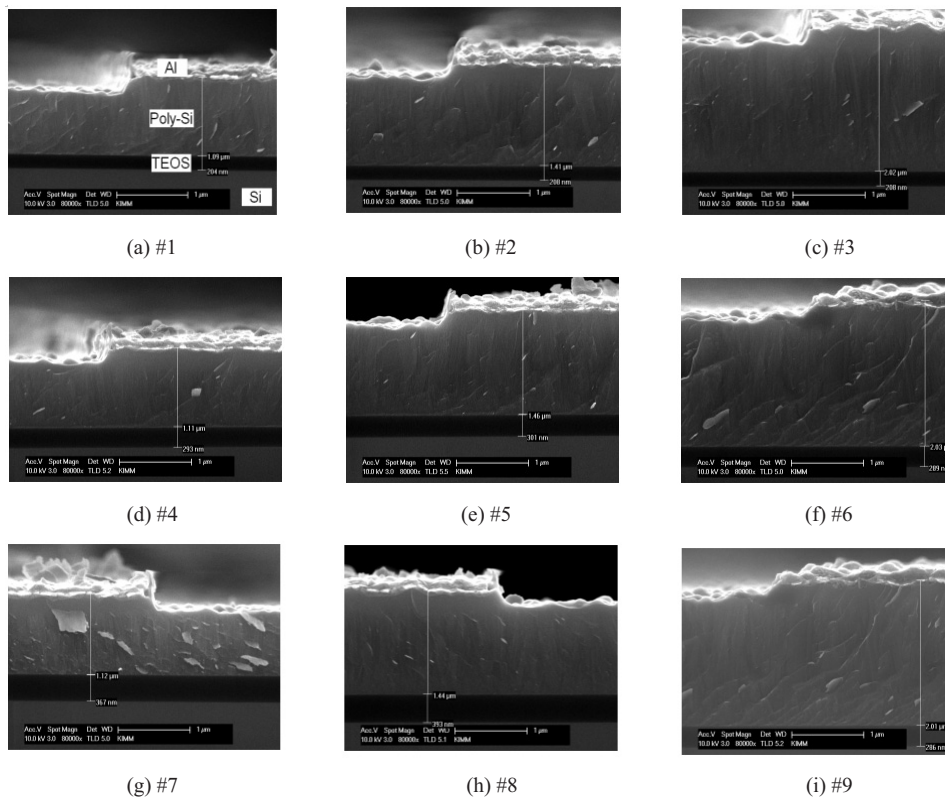


Fig. 2. SEM pictures of the fabricated poly-Si films.

(LPCVD) method on the cleaned wafers. The temperature was 713°C and the flow rate of TEOS gas was 30 sccm under a pressure of 267  $\mu$ bar. The deposition rate was 8.5 nm/min. 0.2, 0.3 and 0.4  $\mu$ m thick TEOS films were obtained in 24, 36 and 48 minutes, respectively. Poly-Si films were grown on the TEOS layer with  $\text{SiH}_4$  gas, whose flow rate was 60 sccm. The deposition was performed at a temperature of 620°C, with a pressure of 200  $\mu$ bar with the LPCVD method. The deposition rate was 8.5 nm/min. 118, 176 and 236 minutes were required for the deposition of 1.0  $\mu$ m, 1.5  $\mu$ m and 2.0  $\mu$ m thick poly-Si layers, respectively.

Subsequently, boron ions were implanted in the poly-Si layers. In this step, each wafer was subjected to different process conditions. The applied energy was varied from 30 keV through 50 keV, and the doses of the dopant were varied from  $10^{14}$   $\text{cm}^{-2}$  through  $10^{16}$   $\text{cm}^{-2}$ .

Additionally, a 0.02  $\mu$ m thick Titanium (Ti) layer was deposited with a power of 500 W, at a chamber temperature of 0°C. A 0.15  $\mu$ m thick aluminum (Al) layer was sputtered on the Ti layer for the fabrication

of the electrode patterns. The supplied power was also 500 W at a temperature of 0°C.

For the patterning of the electrodes, positive photo resist (PR) was coated up to a thickness of 2.0  $\mu$ m. The PR was soft baked for 90 seconds on a 120°C hot plate and then exposed to ultraviolet (UV) light for two seconds through a five inch mask. Then, the PR was developed by using RD6 (TMAH 2.38 w%) for 45 seconds. After developing, a hard baking process was performed. Al and Ti layers were etched for the electrode patterns. After PR stripping, the wafers were cut into 10 mm  $\times$  10 mm (width  $\times$  height) specimens. The SEM pictures of the final specimens are shown in Fig. 2. In each figure, Al/Poly-Si/TEOS layers on the Si substrate can be found. The bright top layers indicate etched Al films. Relatively thick gray layers are poly-Si films. The dark layers between poly-Si layers and Si substrates are TEOS films. Nine combinations of TEOS and poly-Si layers with different thicknesses were also verified. The step shapes in the upper part of each figure were caused by the over-etching of the Al and Ti layers.

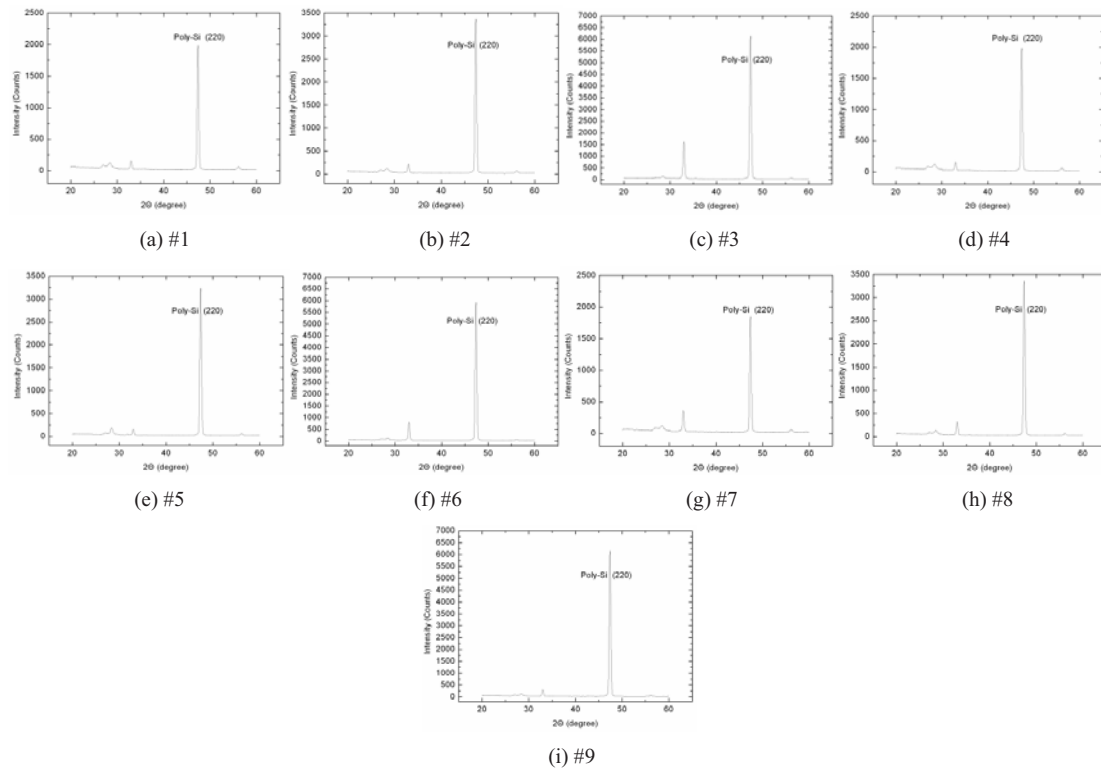


Fig. 3. X-ray diffractometer analysis of the fabricated poly-Si films.

#### 4. Experiments

The crystalline structures of the poly-Si films were observed with an X-ray diffractometer (XRD). The XRD analysis results, shown in Fig. 3, demonstrate that each specimen was crystallized well with the (2 2 0) orientation.

The thermoelectric properties, Seebeck coefficient and electrical conductivity of the specimens were measured. First, the Seebeck coefficient was measured with a Thermoelectric Measurement Setup (Fraunhofer IPM). It is composed of a sample holder with two copper blocks (block A and B), two probe-stations with heads equipped with thermo-elements, two temperature controllers for each copper block, and a digital voltmeter with a scanning card. These devices were operated remotely by a personal computer through an interface. The experimental setup is illustrated in Fig. 4 (a) and (b). The sample holder consisted of two copper blocks that are electro-plated with nickel (Ni) and gold (Au). Two Peltier-elements were used to set a temperature gradient  $\Delta T$  over the sample. The temperatures of the block A  $T_A$  and the

block B  $T_B$  were controlled by two thermoelectric temperature controllers (Thorlabs TED350).  $T_A$  and  $T_B$  were measured with Pt100 temperature sensors. Two probes for measuring the Seebeck coefficient consisted of thermocouples based on copper (Cu) and constantan (Ko). These measurement probes were installed to measure the temperature gradient over the specimen and the resulting thermo-voltage. The temperature gradient and the thermo-voltage were measured with a Keithley Model 2700 equipped with a low-voltage scanning card (Keithley data acquisition system Model 7700). The computer was connected by IEEE-488 cables to the Keithley Model 2700 and to the two temperature controllers cooler A and B.

When setting the condition of the Seebeck coefficient measurement equipment, the environmental temperature was set to be 30°C with a temperature gradient of 10°C.

The electrical conductivity, transport properties, hall coefficient, hall mobility and carrier concentration were measured with a Hall Effect Measurement System (Ecopia Inc.) at room temperature. The applied magnetic flux density was 0.52 T.

The measured Seebeck coefficients are listed in Table 3 and the transport properties in Table 4. They were measured three times and averaged. The maximum Seebeck coefficient was 0.588 mVK<sup>-1</sup>, which was found in the fifth specimen. Positive values of the hall coefficient indicate p-type conductivity. A higher carrier concentration indicates a higher electrical conductivity and lower Seebeck coefficient. The electrical conductivity was good in the fourth specimen, having a value of 3160.7 Ω<sup>-1</sup>m<sup>-1</sup>. The power factors were calculated and are listed in Table 5. The greatest power factor was found in the fourth specimen with a value of 212 μWm<sup>-1</sup>K<sup>-2</sup>.

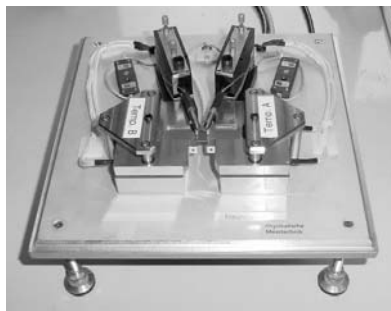
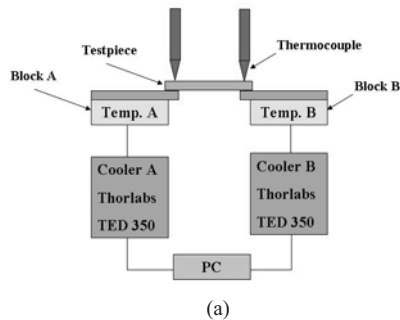


Fig. 4. (a) The schematic description and (b) the picture of the thermoelectric measurement setup.

Table 3. Seebeck coefficient.

No	Seebeck Coefficient, $\alpha$ (mVK <sup>-1</sup> )
1	0.523 ± 0.003
2	0.392 ± 0.019
3	0.277 ± 0.007
4	0.259 ± 0.006
5	0.588 ± 0.001
6	0.382 ± 0.004
7	0.311 ± 0.003
8	0.283 ± 0.004
9	0.523 ± 0.006

### 5. Results and discussion

The average value was calculated for each design parameter and interaction level. First, the responses were grouped by factor level for each column in the array, and then they were summed and divided by the number of responses. The absolute differences between the maximum and minimum values were calculated. The response table was generated as shown in Table 6. The delta values mean the differences between the maximum and minimum values of each factor.

Table 4. Transport properties.

No	Hall Coefficient, $R_H$ (cm <sup>3</sup> C <sup>-1</sup> )	Hall Mobility, $\mu$ (cm <sup>2</sup> V <sup>-1</sup> sec <sup>-1</sup> )	Carrier Concentration, $p$ (cm <sup>-3</sup> )	Electrical Conductivity, $\sigma$ (Ω <sup>-1</sup> m <sup>-1</sup> )
1	59.17	18.86	9.22E+16	20.7 ± 0.7
2	2.08	11.99	3.80E+18	577.3 ± 5.3
3	0.95	21.66	1.27E+19	2330.0 ± 70.0
4	0.44	13.92	1.53E+19	3160.7 ± 180.7
5	15.62	5.77	4.10E+17	37.0 ± 1.8
6	19.01	32.75	3.32E+17	178.4 ± 1.2
7	0.71	8.89	9.02E+18	1262.7 ± 57.7
8	1.55	15.07	4.21E+18	969.0 ± 25.2
9	20.69	8.47	1.04E+16	24.4 ± 0.5

Table 5. Power factor.

No	Seebeck Coefficient, $\alpha$ (mVK <sup>-1</sup> )	Electrical Conductivity, $\sigma$ (Ω <sup>-1</sup> m <sup>-1</sup> )	Power Factor, $\alpha^2\sigma$ (μWm <sup>-1</sup> K <sup>-2</sup> )
1	0.523	20.7	6
2	0.392	577.3	89
3	0.277	2330.0	178
4	0.259	3160.7	212
5	0.588	37.0	13
6	0.382	178.4	26
7	0.311	1262.7	122
8	0.283	969.0	78
9	0.523	24.4	7

Table 6. Response table of the power factors (μWm<sup>-1</sup>K<sup>-2</sup>).

	A	B	C	D
Level 1	91	113	37	8
Level 2	84	60	102	79
Level 3	69	70	105	156
delta	22	54	68	148

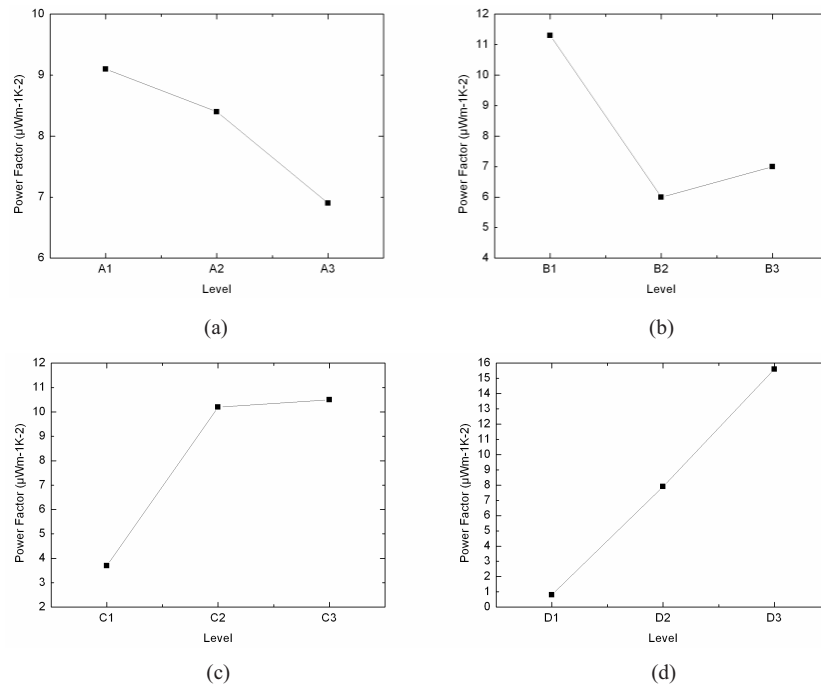


Fig. 5. Response graph of (a) TEOS thickness, (b) poly-Si thickness, (c) energy and (d) dopant dose.

Based on the response table, response graphs were plotted as shown in Fig. 5. The power factor decreased by  $22 \mu\text{Wm}^{-1}\text{K}^{-2}$  as the thickness of the TEOS layer increased from  $0.2 \mu\text{m}$  through  $0.4 \mu\text{m}$ , which is explained in Fig. 5 (a). This result implies that thinner insulation films are preferred to obtain better performance. However, TEOS films with a thickness of at least  $0.2 \mu\text{m}$  are necessary to provide safe insulation between the Si wafer and the thermoelectric layer. The minimum value of  $0.2 \mu\text{m}$  was therefore chosen as a reasonable TEOS thickness. Secondly, the power factor was found to decrease by  $54 \mu\text{Wm}^{-1}\text{K}^{-2}$  when the thickness of the poly-Si films was increased from  $1.0 \mu\text{m}$  to  $1.5 \mu\text{m}$ , as shown in Fig. 5 (b). In contrast, the power factor increased slightly when the thickness was increased to  $2.0 \mu\text{m}$ . Based on these results, it was predicted that better performance would be obtained with the  $1.0 \mu\text{m}$  thick poly-Si films.

Therefore,  $1.0 \mu\text{m}$  was selected as the optimum value. In the doping process, energy of  $50 \text{ keV}$  and a dopant dose of  $10^{16} \text{ cm}^{-2}$  were the optimum conditions, as shown in Figs. 5 (c) and (d), respectively.

Using these optimum values, the power factor was predicted. First, the overall average  $T$  value was calculated as follows:

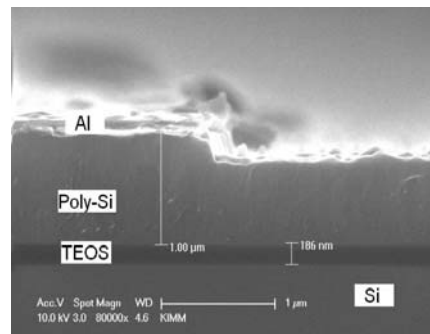


Fig. 6. SEM picture of the optimized poly-Si films.

$$T = (y_1 + y_2 + \dots + y_9) / 9 \quad (2)$$

where  $y_i$  is the power factor of the  $i_{\text{th}}$  specimen, and the predicted power factor can be obtained by using the following equation, which is from Taguchi methods.

$$S_p = T + (A1 - T) + (B1 - T) + (C3 - T) + (D3 - T) \quad (3)$$

where  $S_p$  is the predicted power factor and A1, B1, C3 and D3 are the selected parameter values. The predicted power factor was  $221 \mu\text{Wm}^{-1}\text{K}^{-2}$ . Other

Table 7. Transport properties of the optimized poly-Si films.

Parameters	Hall Coefficient, $R_H$ ( $\text{cm}^3\text{C}^{-1}$ )	Hall Mobility, $\mu$ ( $\text{cm}^2\text{V}^{-1}\text{sec}^{-1}$ )	Carrier Concentration, $p$ ( $\text{cm}^{-3}$ )	Electrical Conductivity, $\sigma$ ( $\Omega^{-1}\text{m}^{-1}$ )
Values	0.88	30.6	$7.09\text{E}+18$	$3471.3 \pm 100.7$

Table 8. Power factor of the optimized poly-Si films.

Parameters	Seebeck Coefficient, $\alpha$ ( $\text{mVK}^{-1}$ )	Electrical Conductivity, $\sigma$ ( $\Omega^{-1}\text{m}^{-1}$ )	Power Factor, $\alpha^2\sigma$ ( $\mu\text{Wm}^{-1}\text{K}^{-2}$ )
Values	$0.395 \pm 0.004$	3471.3	541

poly-Si films were fabricated by using the optimal conditions. The optimized poly-Si films are shown in Fig. 6. There are Pt/Poly-Si/TEOS layers from the top. The measured transport properties are listed in Table 7 and the Seebeck coefficient with the calculated power factor in Table 8. The Seebeck coefficient and electrical conductivity were  $0.395 \text{ mVK}^{-1}$  and  $3471.3 \Omega^{-1}\text{m}^{-1}$ , respectively. The calculated power factor was  $541 \mu\text{Wm}^{-1}\text{K}^{-2}$ , which was higher than the predicted value.

## 6. Conclusion

P-type poly-Si films for micro TEGs were optimized by using an orthogonal array  $L_9$  ( $3^4$ ) based on the Taguchi methods. Nine different poly-Si specimens were fabricated through the semiconductor process. Their power factors were calculated with the measured Seebeck coefficient and electrical conductivity. By analyzing the results, the optimal values of the four design parameters were found. The optimal thicknesses of the TEOS and poly-Si layers were  $0.2 \mu\text{m}$  and  $1.0 \mu\text{m}$ , respectively. The optimal amount of energy in the ion-implantation process and dose of the ions were  $50 \text{ keV}$  and  $10^{16} \text{ cm}^{-2}$ , respectively.

By using the optimal combination of parameters, additional poly-Si films were fabricated for the verification of the experiment. The power factor of these films was  $541 \mu\text{Wm}^{-1}\text{K}^{-2}$ , which was better than the predicted value of  $221 \mu\text{Wm}^{-1}\text{K}^{-2}$ . The obtained optimal condition can be applied to the further development of micro TEGs.

## Acknowledgment

This research was supported by the Fundamental Research Project (NK128E) of the Energy Systems Research Center at the Korea Institute of Machinery and Materials.

## References

- [1] D. M. Rowe, D. V. Morgan and J. H. Kiely, Miniature low-power/high-voltage thermoelectric generator, *Electronics Letters* 25 (1989) 166-168.
- [2] J. J. Kiely, D. V. Morgan and D. M. Rowe, Low cost miniature thermoelectric generator, *Electronics Letters* 27 (1991) 2332-2334.
- [3] M. Strasser, R. Aigner, M. Franosch and G. Wachutka, Miniaturized thermoelectric generators based on poly-Si and poly-SiGe surface micromachining, *Sens. Actuators A* 97-98 (2002) 535-542.
- [4] M. Strasser, R. Aigner, C. Lauterbach, T. F. Sturm, M. Franosch and G. Wachutka, Micromachined CMOS thermoelectric generators as on-chip power supply, *Sens. Actuators A* 114 (2004) 362-370.
- [5] J. Posthill, A. Reddy, E. Siivola, G. Krueger, M. Mantini, P. Thomas, R. Venkatasubramanian, F. Ochoa and P. Ronney, Portable power sources using combustion of butane and thermoelectrics, *Proceedings of International Conference on Thermoelectrics*, Clemson, SC, USA, (2005) 517-520.
- [6] J. K. Kim, Optimum design of a heat-exchanger-fan casing of clothes dryer using the Taguchi method, *KSME International Journal* 13 (12) (1999) 962-972.
- [7] R. S. Chen, C. Kung and G.-B. Lee, Analysis of the optimal dimension on the electrothermal microactuator, *J. Micromech. Microeng.* 12 (2002) 291-296.
- [8] J. Zhang, K. L. Tan, G. D. Hong, L. J. Yang and H. Q. Gong, Polymerization optimization of SU-8 photoresist and its applications in microfluidic systems and MEMS, *J. Micromech. Microeng.* 11 (2001) 20-26.
- [9] G. S. Peace, *Taguchi methods*, Addison-Wesley Publishing Company, (1995).